Reservoir Computing With *in silico* Plants

Maxime Cannoodt

Supervisors: Prof. dr. ir. Francis wyffels, Dr. ir. Michiel Stock
Counselors: Dr. ir. Olivier Pieters, Dr. ir. Tom De Swaef (ILVO)

***Abstract*—We present a framework to evaluate the computational capabilities of plant physiological processes in plant models for physical reservoir computing (PRC). PRC is a computing paradigm that enables the use of physical substrates for computation. Recently, the use of live plants in a PRC context was demonstrated. We expand upon this work *in silico* using plant models for grapevine and wheat. In our experiments, we investigated the use of leaf temperature, transpiration rate, photosynthesis rate, light absorption, water flow, and hydraulic pressure as readout traits. Each of these traits displayed reservoir dynamics and correlated well with biologically relevant tasks. Surprisingly, our framework highlighted unusual behavior in mechanistic plant models, which the authors did not yet report. We propose that the plant-modeling community can adapt the methods in this work to verify the behavior of plant models. We believe that this is just the starting point for plant reservoir computing. If knowledge and technology can scale, there will be countless opportunities in agricultural technology.**

***Keywords*—Physical Reservoir Computing (PRC), Unconventional Computing, Plant Physiology, functional-structural plant models (FSPMs).**

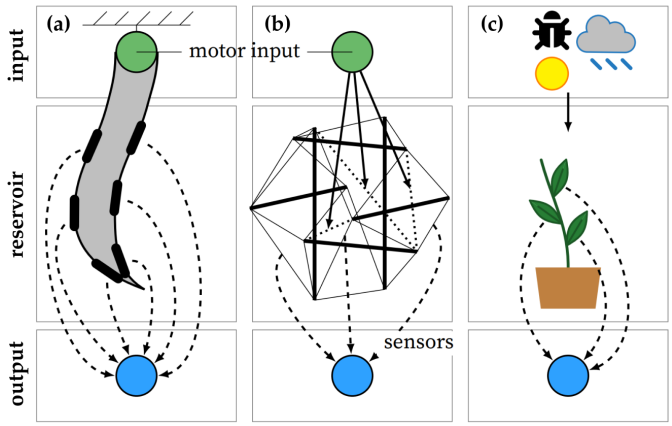

Fig. 1: Illustration of different physical reservoir computing implementations. (a) Bioinspired silicone arm with integrated deformation sensors [6]. (b) Tensegrity robot made of beams and springs [7]. Force sensors measure the dynamics of the spring-mass system. (c) The plant physiological reservoir proposed in this work. Illustration from Pieters (2022)[8] with permission from the author.

I. Introduction

RESERVOIR computing (RC) is a holistic machine learning technique commonly used with time series data. RC is based on the emergent computational properties of nonlinear dynamical systems, the so-called reservoir. The key to understanding reservoir computing is that all non-linearity and memory required to solve a problem are already present in the (observable) reservoir dynamics. These dynamics are combined using a simple linear readout function to obtain the output value for a certain task. RC was first introduced as an alternative to trained recurrent neural networks and as a more biologically plausible computing model [1]–[3]. Later it was observed that two key features of said novel ideas: combining non-linearity and memory, can be identified in many physical systems as well, and there exists a rich literature on the use of physical media as computational resources [4], giving rise the physical reservoir computing (PRC). Here, the reservoir state is partially inferred from sensor data observing the dynamical system from different spatial positions [5], as illustrated in Figure 1.

Plants can also be interpreted as a computational resource. The plant's environment is its input, and its health, growth, and behavior result from processing this information. Interpreting plants as information-processing organisms is not a new idea. A large body of research indicates that plants observe their environment, have memory, and are capable of learning complex patterns [9]. Experiments by Adamatzky et al. have shown limited yet promising success in exploiting plant intelligence to implement various functions and algorithms [10]. Their work serves as experimental evidence that plants can compute highly nonlinear functions. Most recently, Pieters demonstrated the first successful application of reservoir computing with plants [8]. His research shows that *Fragaria* × *ananassa* (strawberry) is capable of performing several environmental, eco-physiological, and computational tasks, paving the way to apply reservoir computing more broadly to a variety of crops.

The work by Pieters has shown that reservoir computing with plants is possible. Now, a more thorough examination of the reservoir dynamics of plant physiological processes is warranted. In this work, we further investigated the reservoir dynamics present in plants. We conducted our research with computer simulations of plants. Working with simulations provided the freedom to observe the plant's physiological processes without the need for sensing technology or laboratory setups. It gives us a first intuition into which processes show promising reservoir dynamics, which informs future research with *in vivo* specimens.

II. Materials and Methods

A. Experimental Design

To perform useful computations, a reservoir must show input separation with regard to the relevant tasks and fading

memory of past environmental conditions [6]. We investigated linear task separation and memory capacity in several observable eco-physiological processes by performing relevant environmental and eco-physiological reservoir tasks. We also verified whether these physiological processes displayed the fading memory property, an essential precondition for performing deterministic computations. We propose an experimental framework for quantitatively measuring these properties in plant physiological processes. The results from these experiments highlight which physiological reservoirs to pursue in future RC research.

1) Input Separation: The reservoir readout is a strictly linear function of the observed reservoir state. So, to perform nonlinear computation, the reservoir must transform its inputs such that the desired task becomes a linear function of the reservoir observations. To measure the input separation with regard to biologically relevant tasks, we used three categories of targets, previously established by Pieters: (i) predicting current environmental conditions, (ii) predicting the plant's eco-physiological performance, and (iii) computational benchmarks. Predicting environmental inputs gives us a first indication of the plant's coupling with the environment. Next, eco-physiological tasks indicate whether the observed reservoir is effective at solving biological problems. Finally, computational benchmarks can measure the reservoir's degree of nonlinearity and memory. We used three benchmarks: a delay line to measure memory capacity, a polynomial expansion to measure nonlinearity, and the Nonlinear Autoregressive Moving Average (NARMA) benchmark, a common benchmark for RC [6]. The NARMA system is defined as:

$$y(t+1) = \alpha y(t) + \beta y(t)\left[\sum_{i=0}^{n-1} y(t-i)\right] + \gamma x(t-n+1)x(t) + \delta \tag{1}$$

where n tunes the nonlinearity and memory of the task and the parameters α, β, γ, and δ are set to 0.3, 0.05, 1.5 and 0.1 [6]. Each computational task uses an environmental input as base signal.

We measured the prediction accuracy of each physiological reservoir for a given task using the normalized mean square error (NMSE) metric:

$$\text{NMSE} = \frac{1}{N}\sum_{t=1}^{N}\frac{(y[t]-\hat{y}[t])^2}{\text{var}(y)} \tag{2}$$

A lower score means a more accurate prediction. The NMSE has several advantages over regular mean square error [8]. Because it is normalized, the results can be compared between reservoir-task pairings, including between plants. It is also easy to interpret: a perfect predictor scores 0.0, while predicting the signal mean for every step yields a score of 1.0.

2) Fading Memory: To perform reliable computations, a reservoir must display the same behavior whenever it is subjected to the same input sequence [11]. In practice, this means past inputs should have a fading influence over the reservoir's present state [12]. The period over which this influence fades forms a trade-off between short-term accuracy and long-term memory. To test fading memory in physiological processes, we designed an experiment in which an impulse is applied to the plant for a brief period, as illustrated in Figure 2. We then compared the trajectory of the physiological reservoir with that of a control experiment that did not receive the impulse. The impulse can be applied to any of the environmental inputs. The amplitude and duration of the impulse should remain within realistic boundaries so that an actual plant would not suffer permanent damage that alters the reservoir dynamics.

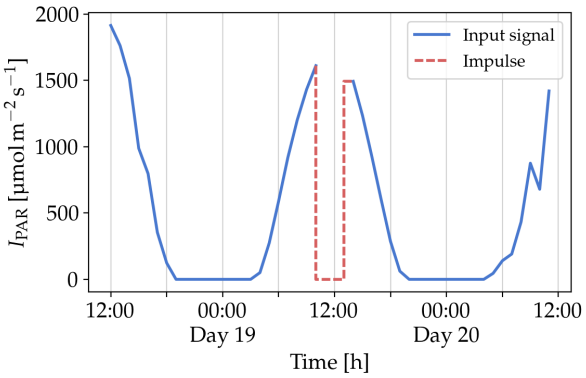

Fig. 2: Applying an impulse of 3 h and a value of 0 µmol m^{-2} s^{-1} to the incident PAR of CN-Wheat.

To quantify the divergence $\delta(t)$ between two reservoir trajectories at a given time step, we used a modified NMSE metric:

$$\delta(t) = \frac{1}{p}\sum_{i=1}^{p}\frac{\left(\mathbf{X}_i^C(t) - \mathbf{X}_i^E(t)\right)^2}{\text{var}\left(\mathbf{X}_i^C\right)} \tag{3}$$

where p is the size of the observed reservoir, $\mathbf{X}^C$ the reservoir state in the control experiment, and $\mathbf{X}^E$ the reservoir state during the impulse experiment. A reservoir affected by the impulse will show a peak in divergence from the control experiment once the impulse is applied. If the physiological process displays fading memory, the divergence should go down to pre-impulse levels in a finite amount of time after the artificial stimulus is removed.

B. Selected Plant Models

We used functional-structural plant models (FSPMs) to test the experimental framework. FSPMs represent the plant as a 3D structure of interconnected elements. Each structural element simulates physiological processes such as photosynthesis, transpiration, and water and carbon flow [13]. This type of model has become the state-of-the-art in plant modeling in the past decade [14].

We present results from two FSPMs: HydroShoot [15] and CN-Wheat [16]. HydroShoot is an FSPM of common grapevine. It was published by Albasha et al. as a study of gas exchange in large plant canopies under water deficit conditions and to compare the effectiveness of different canopy shapes. CN-Wheat, on the other hand, is a mechanistic model of common wheat developed by Barillot et al. The model was made to simulate the effect of fertilization regimes on carbon (C) and nitrogen (N) metabolism in wheat culms during the

post-flowering stages of development. Table I compares the model specifications for the discussed models.

In addition to input separation and fading memory, the PRC framework assumes the reservoir dynamics are unchanging over time. Plants are not static reservoirs in the general case because they go through several growth phases that drastically change their structure and behavior. Because of this, we specifically selected plant models with a static plant structure or a dynamic structure in a stage of post-vegetative growth. For *in vivo* scenarios, stationarity can be approximated by investigating reservoir dynamics within a time window for which the growth rate is negligible [8].

C. Considered Physiological Reservoirs

Many physiological processes inside the plant can be considered a potential reservoir. We limited ourselves to processes that are observable using existing, non-destructive sensing technologies. The observable physiological processes for HydroShoot and CN-Wheat are presented in Table II. We had a preference for processes that are observable using image-based sensors because contactless sensors do not influence the reservoir dynamics [8]. Also, contactless sensing technologies may one day be the key to scaling plant RC to larger arrays of plants. Finally, we did not consider processes that violate fading memory.

D. Reservoir Readout Model

For the reservoir readout function we used a simple linear regression model with a bias term:

$$\hat{y}[t] = w_0 + \sum_{i=1}^{p} w_i x_i[t] \tag{4}$$

Where $\hat{y}$ is the predicted value, x_i the reservoir measurements, and w_i the model parameters. To train the model parameters, we used a gradient descent algorithm to minimize the ridge regularization loss:

$$L_{\text{ridge}} = \frac{1}{N} \sum_{i=0}^{N-1} \left(y[i] - \hat{y}[i]\right)^2 + \lambda \sum_{i=1}^{p} |w_i|^2 \tag{5}$$

where λ is a regularization parameter that prevents overfitting. To find the optimal λ, we used a parameter sweep with logarithmic spacing and a leave-one-out cross-validation scheme. We dedicated 50% of the experimental data for training and cross-validation and the other 50% for testing the final model on unseen data.

TABLE I: Comparison of HydroShoot and CN-Wheat: simulation details.

	HydroShoot	**CN-Wheat**
Simulation step	1 h	1 h
Simulation duration	7 days	50 days
Model structure	static (idealized reservoir)	Post-vegetative growth
Model size	$\approx 10^3$ elements	15 elements

III. Results and Discussion

A. Environmental and Physiological Tasks

We considered air temperature (T_{air}), relative humidity (RH) and incident photosynthetically active radiation (PAR) for the environmental targets. For the physiological targets we used transpiration rate (E), absorbed PAR (Φ_{PAR}) and net photosynthesis rate (A_n). The physiological target A_n was only available for HydroShoot, while both models offer it as a physiological reservoir.

Figure 4a showcases the performance of each physiological reservoir as boxplots. For the HydroShoot model, we observe that each reservoir performs roughly the same for a given target. In CN-Wheat, the difference between the reservoirs is more outspoken. For example, RH correlates relatively well with E in CN-Wheat, where none of the processes in HydroShoot correlate well with RH. We must also note that CN-Wheat significantly outperforms HydroShoot in most tasks.

We study the time series prediction accuracy more closely in Figure 4c. In this figure, we see that the E reservoir captures the broad dynamics of Φ_{PAR} for both HydroShoot and CN-Wheat. However, HydroShoot cannot reproduce finer details, underpredicting the highest targets and overpredicting the lowest. Moreover, HydroShoot's predictions sometimes lag behind the target (Figure 4c, samples A and C), and other times lead the target (Figure 4c, sample D). In contrast, CN-Wheat's transpiration rate captures finer details much better.

B. Computational Benchmarks

We based the computational benchmarks on two different input signals (T_{air} and PAR). For each benchmark, we compared the reservoir's advantage (or disadvantage) over a linear model of the input signal as we increased the benchmark's difficulty. In what follows, we discuss the results for the surface temperature (T_s) and transpiration rate (E) reservoirs specifically.

Figure 4b shows the results for the delay line benchmark. Both reservoirs display memory capacity for this task. The memory for predicting the T_{air} input can be explained by thermal inertia; the difference in heat capacity between air and the plant's water mass results in a slowed reaction to changes in ambient temperature. The readout function can exploit this inertia to learn about past inputs. This is only a first-order interpretation, as it does not consider e.g. heat lost in evaporation. Similarly, thermal inertia can explain the results for incident solar radiation.

Next, Figure 4d presents the accuracy predicting a polynomial expansion. A polynomial relationship exists between air temperature and respiration rate, as the prediction error reaches a minimum for a degree of five. For the other input-reservoir pairings, we see a similar performance characteristic as the linear model plus a bias penalty induced by the noisy input-reservoir relation.

Finally, we consider the NARMA benchmark. In Figure 4f we increased the n parameter from 2 up to 24. For the benchmark based on air temperature, only surface temperature T_s

TABLE II: Comparison of HydroShoot and CN-Wheat: physiological processes observable in each structural element. Not all are shown in the table; we only present the processes that are experimentally observable and that do not violate fading memory. Check marks indicate whether the physiological process is modeled by the FSPM.

Symbol	Description	Unit	HydroShoot	CN-Wheat
A_n	Net photosynthesis rate	$\mu\mathrm{mol\,m^{-2}\,s^{-1}}$	✓	✓
T_s	Surface temperature	$^\circ\mathrm{C}$	✓	✓
g_s	Stomatal conductance	$\mathrm{mol\,m^{-2}\,s^{-1}}$	✓	✓
E	Transpiration rate	$\mathrm{mol_{H_2O}\,m^{-2}\,s^{-1}}$	✓	✓
F	Water flow across segment	$\mathrm{kg\,s^{-1}}$	✓	
Ψ	Mean water potential of segment	MPa	✓	

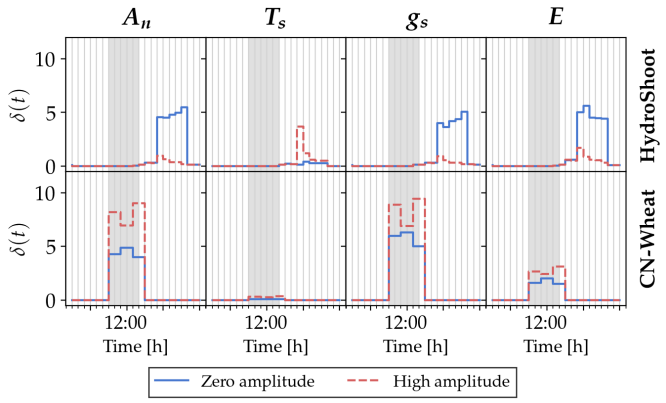

Fig. 3: Predicting a time-delayed signal of T_{air} and PAR using surface temperature (T_s) and transpiration rate (E). The reservoirs' performance is compared to a linear model that uses the benchmark's input as the only feature. The error bars show the scores' standard deviation.

outperformed the linear model. The same thermal inertia theory from before can explain the correlation with this NARMA benchmark. Both T_s and transpiration rate E outperform the linear model for the benchmark based on incident PAR, particularly for n values 8, 12, and 18. The task becomes easier for n equal to 18 and 24. This is because of the averaging effect of Equation 1 as the summation window extends over (nearly) the entire diurnal period of $24\,\mathrm{h}$. Figure 4e shows the time series prediction for the NARMA8 task based on incident PAR, as predicted by surface temperature T_s.

C. Fading Memory

Figure 3 show the divergence $\delta(t)$ (Equation 3) in the physiological reservoirs caused by impulses of $5\,\mathrm{h}$. We applied the impulses to incident PAR with zero and high amplitudes. We used a value of approx. two times the natural maximum signal strength for the high amplitude.

For HydroShoot, the data shows that the reservoir divergence caused by the impulse lasts for the same duration as the impulse itself. However, the reservoir reacts at an $8\,\mathrm{h}$ delay. Investigating the experimental data revealed a continuously shifting misalignment between the diurnal cycle of the input signal and the oscillations in the physiological dynamics. In an extreme case, the peak in transpiration rate lagged nearly a half-period behind the incident PAR. In addition, The data indicates that the reservoir dynamics diverge slightly during the daytime, even between plants subjected to identical conditions. This indicates that the observed physiological processes display somewhat chaotic dynamics during daytime hours. The chaotic behavior may be a result of numerical instabilities in the simulation. However, there exist reports of chaotic behavior in plant physiological responses to light in the literature [17]. The shifting delay in reservoir response is the most likely explanation for the delayed response to the artificial stimulus. We must also attribute the slight disturbance that precedes the peak in divergence to the natural chaotic behavior. After accounting for these two factors, no lasting memory effects are visible at the simulation scale of $1\,\mathrm{h}$; if there are any transient dynamics, they must occur over a much shorter time frame.

The results for CN-Wheat reveal that the simulations responsible for our physiological reservoir update at a $2\,\mathrm{h}$ interval, as described in the model's follow-up paper [18]. Looking past the misalignment caused by the $2\,\mathrm{h}$ simulation step, we see that the reservoir divergence disappears immediately when the real input signal resumes. The most likely explanation is that the transient behavior lasts less than two hours, such that the coarse simulation steps mask any memory effects.

These initial results imply that each considered reservoir has fading memory of incident PAR that lasts less than two hours. Regardless, we can conclude that all reservoirs show stationary behavior w.r.t. this abiotic input.

D. Potential Weaknesses

We used the same measurements for the reservoir as are used by the model to compute the physiological regression tasks. This introduced positive bias into the correlation between the reservoir and the physiological targets. This bias is especially pronounced in the accuracy of CN-Wheat for predicting total transpiration rate and absorbed PAR; CN-Wheat achieves near-perfect accuracy for these tasks. To reduce this bias, we could have introduced some signal noise to the observations to make them less precise. However, it is difficult to determine what amount of noise is appropriate in this case.

Another weakness is the trust in the accuracy of the FSPMs. Plant models are generally not verified as one hundred percent accurate copies of their real-world counterparts. As we described in Section III-C, the HydroShoot model displayed unexpected behavior that was not reported in the original paper. To emphasize that our results characterize the behavior of plant models, we used the names of the FSPMs instead of the plant genus.

Finally, the lack of time resolution in the plant simulations leaves us with a weak take-away about transient memory dynamics in the studied plant species. Though we can conclude that the considered physiological reservoirs show stationary behavior at the hour scale, we cannot state the exact duration during which past inputs influence the present reservoir dynamics.

E. Applications

If plants can behave like reservoir computers, RC may become a versatile addition to the agricultural R&D toolbox. For example, new insights could be gained into eco-physiological processes by observing and measuring the relationship between environmental signals (reservoir input) and plant behavior (reservoir dynamics). We suspect there are many possibilities for discovering new phenomena with this holistic data-driven approach, especially on the time scale between seconds and minutes. In addition, reservoir computing can have applications in phenotyping. The RC framework may identify phenotypes that are better at integrating their environmental inputs into an adaptive response. Especially rapid responses are currently underexplored in phenotyping research, even though they play an essential role in plant life [19], [20]. Even further down the road, RC can find applications in autonomous greenhouses. RC can measure the plant's response to the conditions set by the grower or an autonomous control system in real-time. A closed-circuit control loop could even be designed to let the plant itself controls the delivery of light, water, and nutrients.

IV. Conclusion

Regression benchmarks show promising results for plant RC with several plant physiological processes. In addition, the analysis of fading memory revealed chaotic behavior in physiological processes and unexpected behavior in a plant model that was previously unreported.

To select physiological reservoirs for future research, we recommend cross-referencing our results of reservoir performance with available sensing technologies. For example, surface temperature, transpiration rate, and stomatal conductance form a good combination of reservoir features because they can be observed using thermal cameras [8].

The study of using plants as a substrate for reservoir computing is still in its infancy. There are several yet unexplored topics to extend the foundation of plant RC. We currently only have data on RC with three species: strawberry plants in prior work and now *in silico* versions of grapevine and wheat. Another area that requires attention is how RC can be reconciled with plant growth.

We believe that this is only the beginning of the road for plant reservoir computing. If the knowledge and technology can scale, the opportunities in agricultural tech will be numerous.

References

[1] H. Jaeger, "The "echo state" approach to analysing and training recurrent neural networks - with an erratum note," 2002, [Online]. Available: https://www.ai.rug.nl/minds/uploads/EchoStatesTechRep.pdf.

[2] W. Maass, T. Natschläger, and H. Markram, "Real-time computing without stable states: A new framework for neural computation based on perturbations," *Neural Computation*, vol. 14, no. 11, pp. 2531–2560, Nov. 1, 2002, ISSN: 0899-7667, 1530-888X, DOI: 10.1162/089976602760407955.

[3] J. Steil, "Backpropagation-decorrelation: Online recurrent learning with o(n) complexity," in *2004 IEEE International Joint Conference on Neural Networks (IEEE Cat. No.04CH37541)*, vol. 2, Budapest, Hungary: IEEE, 2004, pp. 843–848, ISBN: 978-0-7803-8359-3, DOI: 10.1109/IJCNN.2004.1380039.

[4] G. Tanaka, T. Yamane, J. B. Héroux, *et al.*, "Recent advances in physical reservoir computing: A review," *Neural Networks*, vol. 115, pp. 100–123, Jul. 2019, ISSN: 08936080, DOI: 10.1016/j.neunet.2019.03.005.

[5] J. Burms, K. Caluwaerts, and J. Dambre, "Reward-modulated hebbian plasticity as leverage for partially embodied control in compliant robotics," *Frontiers in Neurorobotics*, vol. 9, Aug. 17, 2015, ISSN: 1662-5218, DOI: 10.3389/fnbot.2015.00009.

[6] K. Nakajima, H. Hauser, T. Li, and R. Pfeifer, "Information processing via physical soft body," *Scientific Reports*, vol. 5, no. 1, p. 10 487, Sep. 2015, ISSN: 2045-2322, DOI: 10.1038/srep10487.

[7] K. Caluwaerts, M. D'Haene, D. Verstraeten, and B. Schrauwen, "Locomotion without a brain: Physical reservoir computing in tensegrity structures," *Artificial Life*, vol. 19, no. 1, pp. 35–66, Jan. 2013, ISSN: 1064-5462, 1530-9185, DOI: 10.1162/ARTL_a_00080.

[8] O. Pieters, "Reservoir computing with plants," Ph.D. dissertation, Ghent University. Faculty of Engineering and Architecture, 2022, 235 pp., [Online]. Available: http://hdl.handle.net/1854/LU-8739713.

[9] S. Mancuso, *The revolutionary genius of plants: a new understanding of plant intelligence and behavior*, First Atria books hardcover edition. New York, NY: Atria Books, an imprint of Simon & Schuster, Inc, 2018, 225 pp., OCLC: on1048600309, ISBN: 978-1-5011-8785-8.

[10] A. Adamatzky, S. Harding, V. Erokhin, *et al.*, "Computers from plants we never made: Speculations," in *Inspired by Nature*, S. Stepney and A. Adamatzky, Eds., vol. 28, Series Title: Emergence, Complexity and Computation, Cham: Springer International Publishing, 2018, pp. 357–387, ISBN: 978-3-319-67996-9 978-3-319-67997-6, DOI: 10.1007/978-3-319-67997-6_17.

[11] K. Nakajima, "Physical reservoir computing—an introductory perspective," *Japanese Journal of Applied Physics*, vol. 59, no. 6, p. 060 501, Jun. 1, 2020, ISSN: 0021-4922, 1347-4065, DOI: 10.35848/1347-4065/ab8d4f.

[12] M. Lukoševičius, H. Jaeger, and B. Schrauwen, "Reservoir computing trends," *KI - Künstliche Intelligenz*, vol. 26, no. 4, pp. 365–371, Nov. 2012, ISSN: 0933-1875, 1610-1987, DOI: 10.1007/s13218-012-0204-5.

[13] J. R. Coussement, T. De Swaef, P. Lootens, and K. Steppe, "Turgor-driven plant growth applied in a soybean functional–structural plant model," *Annals of Botany*, vol. 126, no. 4, pp. 729–744, Sep. 14, 2020, ISSN: 0305-7364, 1095-8290, DOI: 10.1093/aob/mcaa076.

[14] G. Louarn and Y. Song, "Two decades of functional–structural plant modelling: Now addressing fundamental questions in systems biology and predictive ecology," *Annals of Botany*, vol. 126, no. 4, pp. 501–509, Sep. 14, 2020, ISSN: 0305-7364, 1095-8290, DOI: 10.1093/aob/mcaa143.

[15] R. Albasha, C. Fournier, C. Pradal, *et al.*, "HydroShoot: A functional-structural plant model for simulating hydraulic structure, gas and energy exchange dynamics of complex plant canopies under water deficit—application to grapevine (vitis vinifera)," *in silico Plants*, vol. 1, no. 1, diz007, Jan. 1, 2019, ISSN: 2517-5025, DOI: 10.1093/insilicoplants/diz007.

[16] R. Barillot, C. Chambon, and B. Andrieu, "CN-wheat, a functional–structural model of carbon and nitrogen metabolism in wheat culms after anthesis. II. model evaluation," *Annals of Botany*, vol. 118, no. 5, pp. 1015–1031, Oct. 2016, ISSN: 0305-7364, 1095-8290, DOI: 10.1093/aob/mcw144.

[17] S. Shabala, R. Delbourgo, and I. Newman, "Observations of bifurcation and chaos in plant physiological responses to light," *Functional Plant Biology*, vol. 24, no. 1, p. 91, 1997, ISSN: 1445-4408, DOI: 10.1071/PP96075.

[18] R. Barillot, C. Chambon, and B. Andrieu, "CN-wheat, a functional–structural model of carbon and nitrogen metabolism in wheat culms after anthesis. i. model description," *Annals of Botany*, vol. 118, no. 5, pp. 997–1013, Oct. 2016, ISSN: 0305-7364, 1095-8290, DOI: 10.1093/aob/mcw143.

[19] J.-J. Alarcon and M. Malone, "Substantial hydraulic signals are triggered by leaf-biting insects in tomato," *Journal of Experimental Botany*, vol. 45, no. 7, pp. 953–957, 1994, ISSN: 0022-0957, 1460-2431, DOI: 10.1093/jxb/45.7.953.

[20] T. De Swaef, K. Vermeulen, N. Vergote, *et al.*, "Plant sensors help to understand tipburn in lettuce," *Acta Horticulturae*, no. 1099, pp. 63–70, Sep. 2015, ISSN: 0567-7572, 2406-6168, DOI: 10.17660/ActaHortic.2015.1099.3.

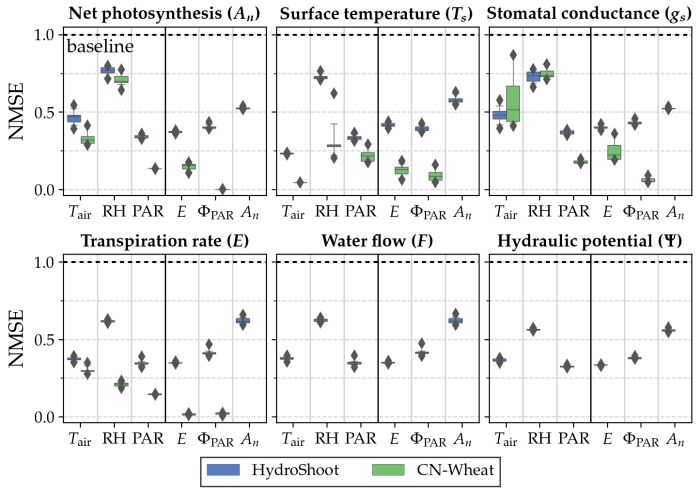

(a)

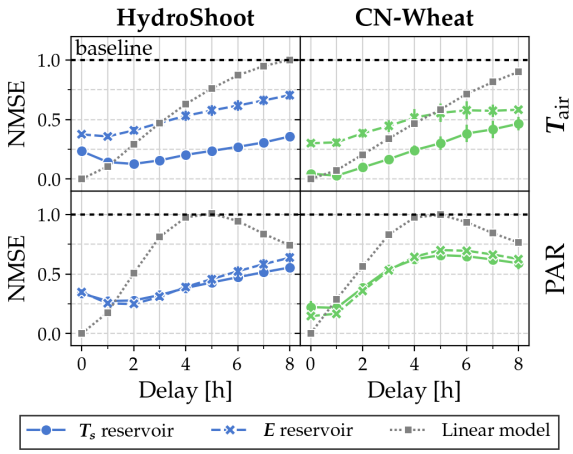

(b)

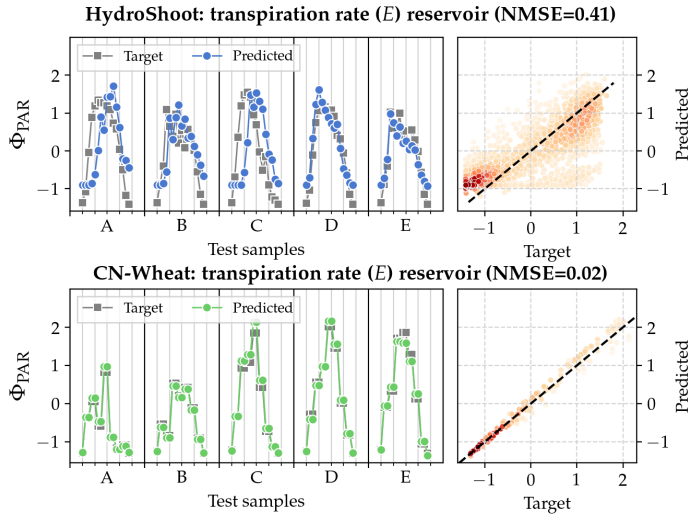

(c)

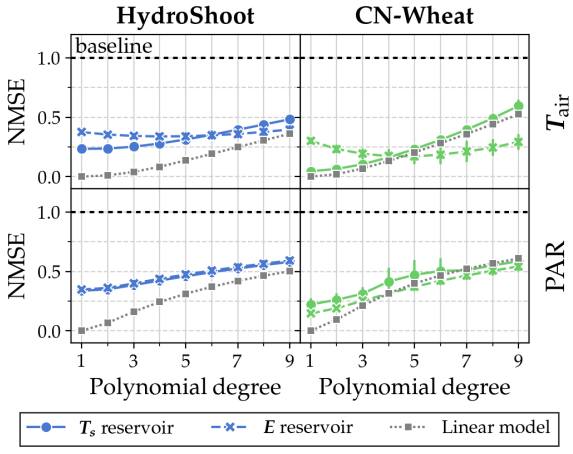

(d)

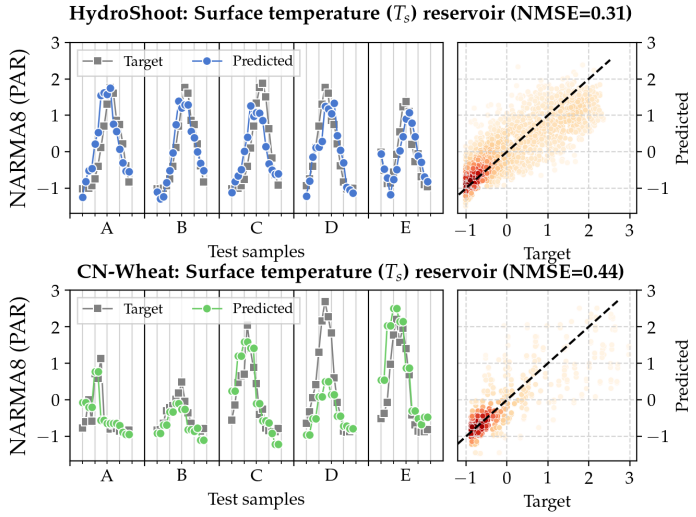

(e)

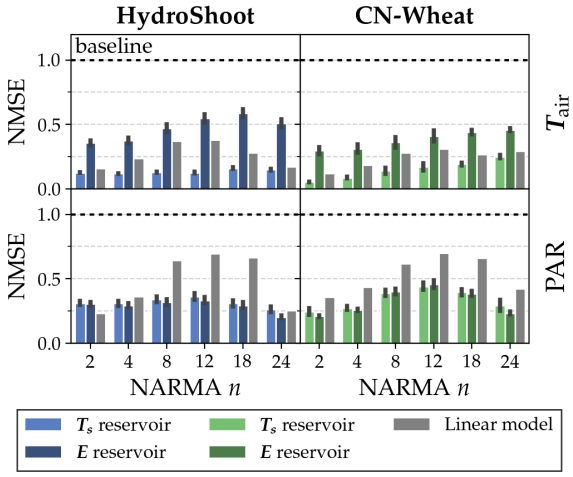

(f)

Fig. 4: Results for input, physiological, and computational tasks. Each figure shows the distribution of test scores for 16 random reservoir samplings. (a): Reservoir performance for input and physiological regression tasks. The plots show prediction accuracy for a suite of regression tasks for each of the physiological reservoirs from Table II. The regression target of net photosynthesis rate A_n was only available for the HydroShoot model. The box shows the quartiles of the distribution; the whiskers indicate the 5th and 95th percentiles. (b, d, f): Predicting a delayed signal, polynomial expansion, and NARMA task based on T_{air} and PAR using surface temperature (T_s) and transpiration rate (E). The reservoirs' performance is compared to a linear model that uses the benchmark's input as the only feature. The error bars show the scores' standard deviation; (c, e): Time series prediction of absorbed PAR and NARMA8 using E and T_s, respectively. The left plot shows predictions for five days randomly sampled from the test set. the right shows correlation between target and predicted values. Darker colors indicate a greater density of points.